

A Record of Change in Oyster Environment through High-Resolution Geochemical Analysis of Late Holocene Sediments from Coastal Ghana

Edem Mahu^{1,*}, Melanie J. Leng², Luke Andrews^{3,4}, Apichaya Englong⁵, and Robert Marchant³

1. Department of Marine and Fisheries Sciences, University of Ghana, Accra, Ghana

2. British Geological Survey, Keyworth, Nottingham NG12 5GG, UK and School of Biosciences, University of Nottingham, Loughborough LE12 5RD

3. Department of Environment and Geography, University of York, York YO10 5DD, North Yorkshire, UK

4. Climate Change Ecology Research Unit, Faculty of Geographical and Geological Sciences, Adam Mickiewicz University, Poznan, Poland

5. Biological Sciences Program, Department of Botany, Chulalongkorn University, Bangkok, Thailand

*Corresponding author: emahu@ug.edu.gh

Abstract

The near-coast environments where oysters occur are among the most impacted by humans globally, especially during the Late Holocene. Yet, in West Africa, there is no documented historical record of change in these environments. We provide insight into the changing geochemical conditions of two oyster environments through high-resolution analysis of total organic carbon (C), total nitrogen (N), carbon and nitrogen isotope ratios ($\delta^{13}\text{C}$, $\delta^{15}\text{N}$), and trace elements, in two cores retrieved from the Densu estuary and the Anyanui-Keta Creek in Ghana. Drastic shifts in sedimentation rate occurred in the Keta and Densu cores around 1996 CE and 960 CE respectively. At these times, comparatively, low levels of C and N were found in the Densu core. Increasing C and N levels and decreasing $\delta^{13}\text{C}$ upcore aligned with the observed shift in sedimentation rate in the Keta core. The C/N ratios in the Keta core suggest allochthonous organic matter (OM) dominance in the creek. The Densu core showed periodic changes in C/N ratios from very high values (>20) between 1918 BCE and 1321 BCE, to values between 20 and 11 between 1321 BCE and 1977 CE and below 10 from the late 1970s CE to the present day, suggesting a varying degree of transformation in the catchment basin. Extremely high Sulfur (S) and moderate to significant Iron (Fe) increases suggest reducing conditions in the Keta sediments. Moderate Calcium (Ca), Zinc (Zn), and Strontium (Sr) concentrations in the upper part of the Densu core suggest a stronger influence of marine processes in the Densu in recent times. The findings reflect the impacts of catchment basin modification on the health of the two coastal environments, likely to impact the growth, productivity, and sustainability of the fishery of the West African mangrove Oyster.

Keywords. Sedimentation, organic matter, marine processes, land-use/landcover change, reduction processes, Oyster fishery, sustainability.

45
46
47
48

1.0 INTRODUCTION

49 Oyster fisheries contribute significantly to the well-being and livelihood needs of artisanal
50 coastal communities in West Africa (Mahu et al., 2022). For many years, the oyster fishery,
51 dominated by women, has sustained vulnerable communities across coastal West Africa and
52 continues to remain relevant in the context of food security, poverty alleviation, health, and
53 well-being, and supporting gender balance. All these factors contribute directly to attaining
54 the UN Sustainable Development Goals. Within the context of ecosystem systems services,
55 oysters contribute significantly to improving environmental health, protecting coastlines, and
56 mitigating climate change, thus featuring significantly in the goals of the United Nations
57 Ocean decade for sustainable development (2021-2030). Despite these numerous societal
58 and ecosystem benefits, oyster populations have declined globally due to various
59 anthropogenic pressures (Zu Ermgassen et al., 2020). More than 85% of oyster reefs have
60 been lost to habitat degradation, water quality impairment, climate change, and mangrove
61 deforestation, ranking them among the most threatened ecosystems on our planet today
62 (Beck et al., 2011).

63

64 Oyster environments comprise nearshore ecosystems such as estuaries, lagoons, and
65 mangrove ecosystems. These environments are highly dynamic but also complex and
66 challenging due to constantly changing conditions (Montagna et al., 2012). Large variations in
67 geochemical conditions often driven by catchment area modifications profoundly affect
68 oyster growth, reproduction, productivity, and survival (North et al., 2010). Landcover
69 removal and other land use changes accelerate the influx of sediments, organic matter,
70 nitrogen, and trace elements to such transitional environments, thereby, altering their
71 natural cycling, and creating undesirable impacts on the ecosystem (Kennish, 2002). While
72 the flux of organic matter into coastal ecosystems is important for food web dynamics and
73 productivity (Bernoux et al., 1998), an excessive supply of organic matter could compromise
74 estuarine health. For instance, marine primary production typically removes CO₂ from surface
75 water, thereby decreasing ocean acidification, and adding this carbon as organic matter to
76 bottom waters (Capelle et al., 2020). Microbial breakdown of organic matter in bottom waters
77 releases CO₂, consequently lowering the bottom water pH (Hopkinson et al., 1998). Notably,
78 carbon cycling in the marine environment promotes aragonite under-saturation and pCO₂
79 elevation everywhere except in surface waters, with the most significant impacts in bottom
80 waters (Capelle et al., 2020). For bottom-dwelling shellfish such as oysters, a lower aragonite
81 under-saturation state results in difficulties in shell building, leading to shell thinning, reduced
82 growth rate, and increased mortality (Gazeau et al., 2011). Another consequence of high
83 organic matter levels is the removal of dissolved oxygen through microbial respiration
84 (Wallace et al., 2014), resulting in low dissolved oxygen levels. Stress from low dissolved
85 oxygen can yield profound lethal and sublethal effects on many species, including oysters,

86 leading to reduced growth, reduced feeding, and increased susceptibility to disease (Baker
87 and Mann, 1994; David et al., 2005; Patterson et al., 2014).

88

89 The C/N ratios allow source determination of organic matter in estuarine ecosystems,
90 providing insight into how much influence estuaries and other nearshore coastal ecosystems
91 receive from fluvial or marine processes (Perdue and Koprivnjak, 2007). Typically, C/N ratios
92 between 4 and 10 indicate dominant marine influence or in-estuary productivity, whereas
93 ratios greater than 20 depict largely fluvial processes and terrestrial organic matter influx into
94 coastal ecosystems (Andersson et al., 2012). The $\delta^{13}\text{C}$ and $\delta^{15}\text{N}$ reflect both salinity and
95 productivity variabilities in coastal ecosystems, thereby, helping to discriminate between
96 fluvial and marine processes (Medina and Francisco, 1997). Salinity is an important ecological
97 factor in oyster growth and health. Changes in salinity have profound effects on the
98 physiology of oysters including altered filtration and respiration rates, growth, reproduction,
99 and mortality (Sutton et al., 2012; Yankson, 1990; Sutton and Yankson, 2007). Estimates of
100 C/N ratios combined with $\delta^{13}\text{C}$ and $\delta^{15}\text{N}$ are important proxies for understanding historical
101 changes in salinity and nutrient regimes in oyster environments while deepening our
102 understanding of the impacts of watershed hydrological modifications on the environmental
103 health of oysters and the fisheries surrounding these (Leng et al., 2017).

104

105

106 While the health of oyster environments globally has been reported to be on the decline, the
107 availability of historical data on how these environments in West Africa have changed is
108 unknown due to limited research. High-resolution, long-term historical data on estuarine
109 geochemistry do not exist. This paucity of estuarine biogeochemical data constrains our
110 understanding of what is changing in oyster environments, the extent and magnitude of the
111 change, and possible consequences to livelihoods and ecosystem services. The present study
112 used variabilities in trace elements (Al, Si, K, Ti, Ca, Fe, Rb, Zn, Sr, Zr, Mn), C and N, (C/N ratios),
113 $\delta^{13}\text{C}$, and $\delta^{15}\text{N}$ to look for geochemical changes in oyster environments in Ghana over the past
114 ~3000 years. Although the data presented has wider implications for coastal ecosystem
115 health, this paper will discuss findings in relation to oyster health and productivity in West
116 Africa.

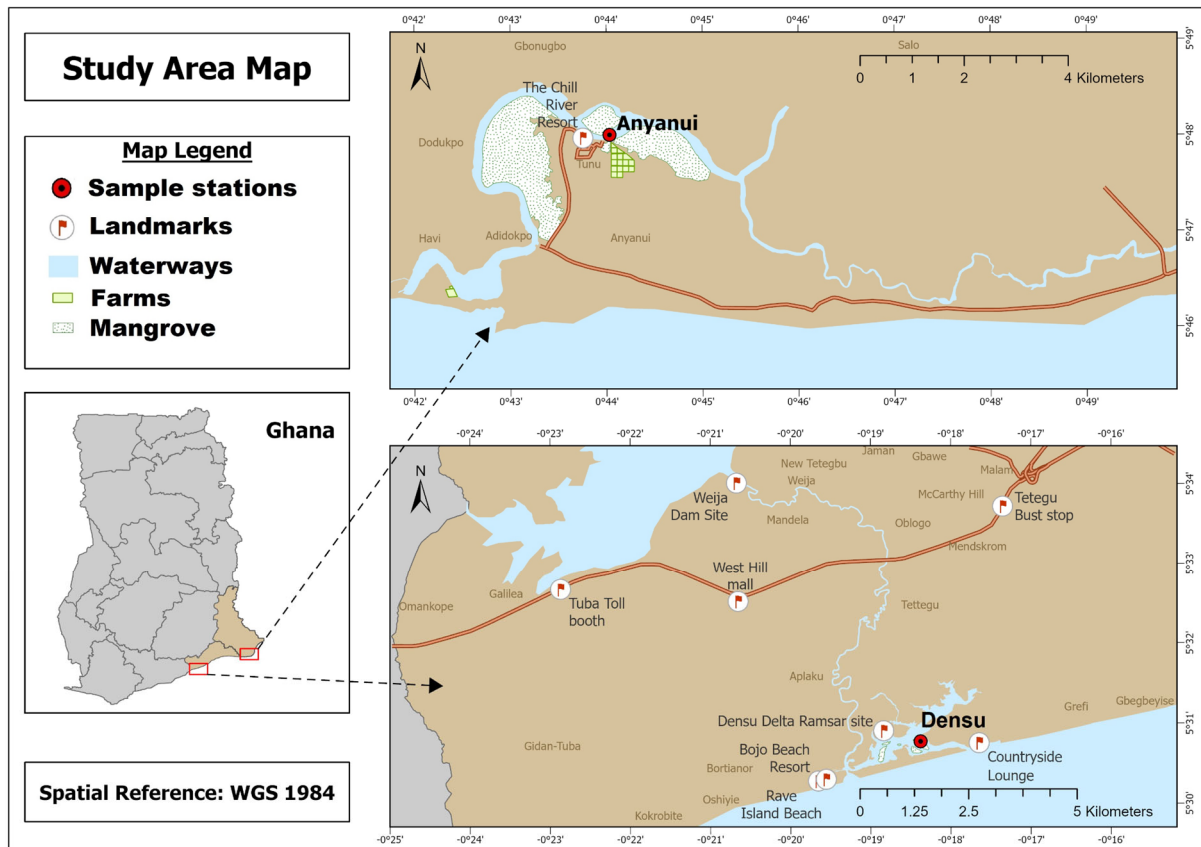
117

118 2.0 MATERIALS AND METHODS

119 Sediment Coring and Preparation

120 Two sediment cores 150 cm and 200 cm in length were retrieved in December 2021 from the
121 mouth of the Densu Estuary (Densu core) and Keta-Anyanui Creek (Keta core) respectively
122 (Fig. 1) Located in the urbanized region of Ghana's capital, the Densu Estuary connects the
123 Densu River to the Atlantic Ocean and supports healthy populations of the West African
124 Mangrove Oyster *Crassostrea tulipa*. Due to its location, the Densu estuary, a Ramsar site, has

125 experienced significant historical land-use and land cover changes in its catchment, with
126 significant growth in the built-up environment (Adjei et al., 2019). The Anyanui Creek, a
127 tributary of the Volta estuary connects the Volta River, the Keta Lagoon, and the Atlantic
128 Ocean. The Creek is situated in a dense mangrove forest in the Anloga District in the Volta
129 Region. Unlike the Densu Estuary, the catchment basin of Anyanui Creek is less urbanized,
130 however, there is evidence of fertilizer-intensive farming and trading of mangrove wood for
131 livelihood purposes (Mahu et al., 2023). Significant land-cover transformations in the Keta
132 area between 1991 and 2020 are linked to increased cutting of mangroves for fuel wood and
133 fishing traps and clearing the land for agricultural purposes (Duku et al., 2021). The Creek
134 which once recorded a very healthy oyster population is currently witnessing a decrease in
135 the oyster population with remaining populations showing signs of stress including poor
136 growth, and thin and fragile shells. The two cores were collected using a 5 cm diameter x 50
137 cm length Russian-type corer. Cores were collected in 50 cm sections from overlapping
138 adjacent boreholes with a 10 cm overlap between core sections. On retrieval, sediments were
139 transferred to a PVC pipe and wrapped in aluminum foil ahead of transportation to cold
140 storage. The sediment cores were stored at 4°C until ready for analysis. Each core was sub-
141 sectioned at 1 cm intervals and dried to constant weight at 60 °C for all analyses except for
142 trace element scans which were carried out on whole cores. The porosity and dry bulk density
143 were determined at the Department of Environment and Geography Laboratories of the
144 University of York.



145
 146 Figure 1: Map of sampling areas in the Densu Estuary and the Anyanui Creek, Ghana
 147

148 Radiocarbon Dating of Cores and Sedimentation Rates.

149 Chronologies were developed for each core through the analysis of organic samples (tree bark
 150 and charcoal) isolated from selected depths within each core. The organic samples were
 151 treated with acid–base–acid (ABA) solution following Brock et al. (2010), to remove soluble
 152 carbonates and prevent humic acids from percolating into the sediment sequences. The pre-
 153 treated samples were radiocarbon-dated by Acceleration Mass Spectrophotometry (AMS) at
 154 the DirectAMS Radiocarbon Dating Facility (Washington, USA). For the Keta core radiocarbon
 155 dates were obtained at 50 cm, 100 cm, 150 cm, and 200 cm depths, whereas for the Densu
 156 core, dates were obtained at 100 cm and 150 cm depths. We **did not** date the 50 cm depth of
 157 the Densu core because the prepared samples **did not** have any charcoal or tree bark material.
 158 Age–depth models were constructed using Oxcal 4.4 software (Ramsey, 2009; Ramsey, 1995)
 159 by applying the P-Sequence function, assuming $k_0 = 1$. This method uses information about
 160 the order and position of dates within a sequence to constrain posterior age distributions to
 161 provide interpolated age range estimates for any given depth (here: 1 cm slices) within a
 162 modeled core. Outlier dates were omitted from the model based on the Agreement Index

163 (Ramsey, 1995), an indicator of the overlap between prior data and the posterior model.
164 Samples were omitted should their agreement index and the overall model be below 60%.
165 Radiocarbon dates were calibrated using the IntCal20 (Reimer et al., 2020) and BombNH2
166 (Hua et al., 2022) curves for samples dated before and after the year 1950 respectively.
167 Calibrated dates referenced in this study are the mean of the posterior distribution for
168 readability and are reported as BCE/CE.

169

170 **C, N, C/N ratio, $\delta^{13}\text{C}$ and $\delta^{15}\text{N}$**

171 Analysis of C, N, $\delta^{15}\text{N}$ and $\delta^{13}\text{C}$ was carried out at the National Environmental Isotope Facility
172 at the British Geological Survey (Nottingham, UK). Oven-dried sediment was analyzed for C
173 and N using a Carlo-Erba CN analyzer, while $\delta^{15}\text{N}$ and $\delta^{13}\text{C}$ were measured using an Elementar
174 Vario ISOTOPE cube elemental analyser (EA) coupled to an Isoprime precisiON isotope ratio
175 mass spectrometer (IRMS) with an onboard centriON continuous flow interface system. The
176 EA inlet converts organic materials in solid sample matrices into pure gases via high-
177 temperature combustion. The post-combustion gas mixture is then separated and focused
178 into individual molecular species for quantitative nitrogen and carbon content analysis. It is
179 then passed online to the mass spectrometer to determine the stable isotope composition.
180 The $\delta^{13}\text{C}$ and $\delta^{15}\text{N}$ data are reported in delta (δ) notation in per mill (‰) relative to the
181 international reference scales VPDB and AIR, respectively. $\delta^{13}\text{C}$ data were corrected using a
182 two-point calibration against organic analytical standard B2162 (spirulina, Elemental
183 Microanalysis Ltd.; -18.7‰) and a laboratory working standard (BROC3, -27.6‰). $\delta^{15}\text{N}$ datas
184 were corrected using a multi-point calibration to USGS40 (-4.5‰), USGS41 ($+47.6\text{‰}$), B2162
185 ($+6.1\text{‰}$), and BROC3 ($+1.5\text{‰}$). The laboratory reference material BROC3 and B2162 have
186 been calibrated for $\delta^{13}\text{C}$ using IAEA-CH-6 (-10.4‰), USGS54 (-24.4‰), USGS40 (-26.4‰),
187 and B2174 (urea, Elemental Microanalysis Ltd.; -36.5‰), and for $\delta^{15}\text{N}$ using USGS40 (-4.5‰),
188 IAEA-N-1 ($+0.4\text{‰}$), and IAEA-N-2 ($+20.3\text{‰}$). BROC3 (41.3 %C and 4.9 %N) was used to
189 calculate the carbon and nitrogen elemental content of samples and C/N is reported as the
190 mass ratio. External precision (1σ) for the within-run standards and sample repeats was
191 $\leq 0.1\text{‰}$ for both $\delta^{13}\text{C}$ and $\delta^{15}\text{N}$.

192

193

194

195 **Trace Element Analysis**

196 Trace element analysis was carried out at Manor Hall, Department of Archeology, University
197 of York using a high-resolution Handheld Olympus Delta XRF, DPO2000 set to geochemical
198 mode. Each core was scanned at 1 cm intervals until 50 cm, after which scans were made at
199 10 cm intervals up to the oldest regions. This sampling strategy was adopted due to time
200 constraints that prevented the full length of each core from being analysed at a high
201 resolution. Instead, we concentrated the high-resolution analyses on the uppermost section
202 of the core, assuming this would contain the most intense periods of anthropogenic activity
203 relevant to the past few centuries. Lower resolution analysis was carried out throughout the
204 rest of the core, allowing us to assess natural variability and characterize conditions before
205 significant levels of disturbance. Both cores were scanned for a wide array of elements;
206 however, only major elements Al, Si, K, Ti, Ca, and Fe, and minor elements Rb, Zn, Sr, Zr, and
207 Mn were detected in the cores. For each core, standards (i.e., silicon) and standard reference
208 material (SRM 2711a) were analyzed between scans. Overall, eighteen SRM 2711a were
209 analyzed for both cores. Recoveries ranged from 72.4% for Ca to 130.3% for Zn.

210

211 **Estimation of Geochemical Enrichment Factors**

212 The enrichment factor evaluates the control of anthropogenic processes on trace metal
213 accumulation in sediments by differentiating between metals originating from anthropogenic
214 sources and those originating from natural sources (Raj and Jayaprakash, 2008). Estimation
215 of trace metal enrichment factor helps to deal with variabilities in trace element
216 concentration associated with natural geochemical factors including grain size effect. It
217 normalizes the measured trace element concentration in the sample with respect to a sample
218 reference element such as Al, Fe, or Ti (Raj and Jayaprakash, 2008).

219

220 The element Al was used as the sample reference element in this study since its concentration
221 is derived majorly from natural processes and it is considered one of the most abundant
222 elements in the upper continental crust (Raj and Jayaprakash, 2008). The enrichment factors
223 were estimated from Equation 1.

224
$$EF = \left[\frac{C_i}{C_{ie}} \right] S / \left[\frac{C_i}{C_{ie}} \right] RS$$

1

225 where C_i is the element under consideration, the square brackets indicate concentration
 226 (usually in mass/mass units, such as mg/kg), C_{ie} is a reference element, S is the sample of
 227 interest and RS is the reference sample. Upper continental crust (Taylor and McLennan, 1995)
 228 was chosen as the reference material for this study. The enrichment factor is interpreted
 229 using five categories of enrichment values: $EF < 2$, implying depletion to mineral or natural
 230 enrichment; $2 \leq EF < 5$, implying moderate enrichment; $5 \leq EF < 20$, implying significant
 231 enrichment; $20 \leq EF < 40$; implying very high enrichment; and $EF > 40$, implying extremely high
 232 enrichment in the sediments (Taylor and McLennan, 1995)

233
 234

235 3.0 RESULTS

236 Radiocarbon Dates, Age-Depth Model, and Sedimentation Rates

237 The results of the radiocarbon dating are presented in Table 1 and the modeled chronology
 238 for each core is presented in Figure 2. The 150 cm long Densu core was aged to 3997 ± 28
 239 years BP whereas the 200 cm long Keta core was aged to 1952 ± 29 years BP. For the Keta
 240 model, an initial run showed poor model agreement (30.2 %) caused by low agreement
 241 between samples at 200 cm and 250 cm depths, likely due to the penetration of younger
 242 mangrove roots. Removal of these samples greatly enhanced the agreement between priors
 243 and posterior data (92.8 %); therefore, this was the model that we chose to use in this study.
 244 This model indicates that rapid accumulation occurred at approximately 100 cm (1996 CE) to
 245 the top of the core, with a mean modeled sedimentation rate of 4 cm/year. Before this, the
 246 sedimentation rate was 0.3 cm/year from 1823 CE to 1992 CE and 0.03 cm/year from 62 CE
 247 to 1820 CE.

248

249 Table 1: Radiocarbon and IntCal20 calibrated Ages of the Keta and Densu cores retrieved
 250 from the Anyanui Creek and Densu Estuary Respectively.

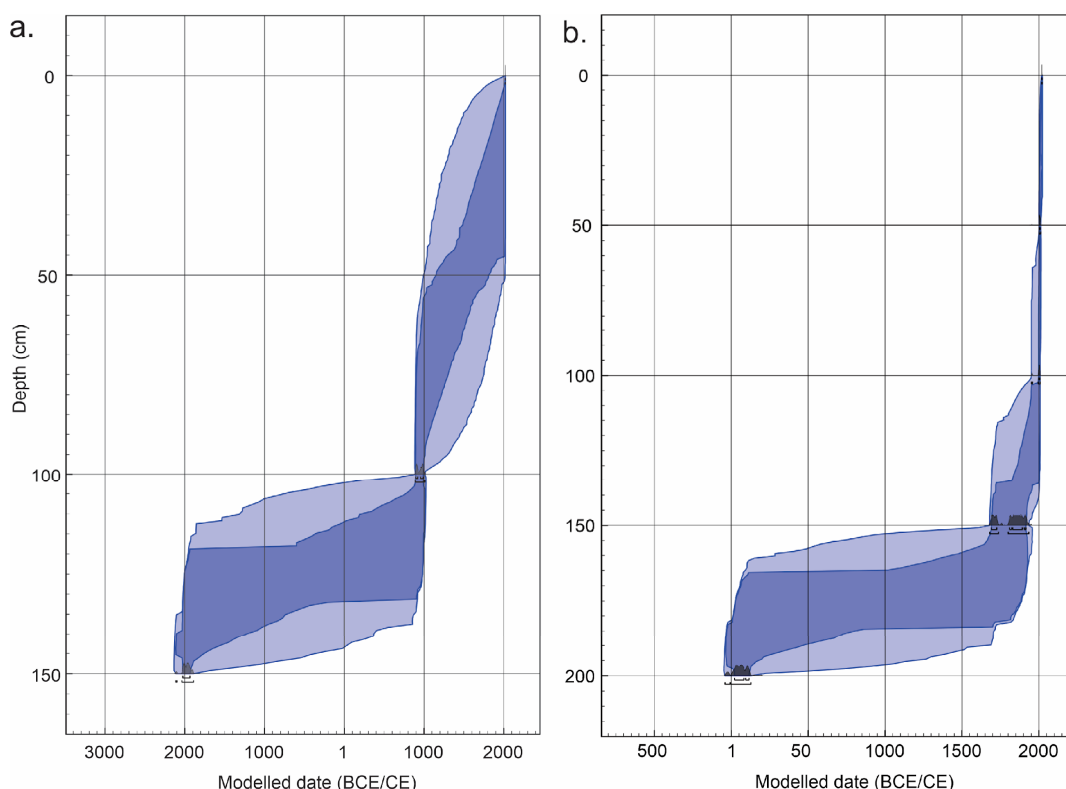
251

Lab Code	Core ID	Depth (cm)	Sample Type	Fraction modern C		Radiocarbon age		Calibrated Ages (Years BP)
				pMC	1 σ error	BP	1 σ error	
D-AMS 046340	KETA	50	Tree bark, charcoal	105.82	0.39	Modern		14 ± 1
D-AMS 046341	KETA	100	Tree bark, charcoal	107.78	0.34	Modern		25 ± 3
D-AMS 046342	KETA	150	Tree bark, charcoal	98.54	0.27	118	22	201 ± 22
D-AMS 046343	KETA	200	Tree bark, charcoal	78.32	0.28	1963	29	1952 ± 29

D-AMS 046345	DENSU	100	Tree bark, charcoal	87.29	0.25	1092	23	1072 ± 23
D-AMS 046346	DENSU	150	Tree bark, charcoal	63.75	0.22	3616	28	3997 ± 28

252
253
254
255
256
257

The Densu model showed far better agreement (99.1 %). Just like the Keta core, there is a similar rapid increase in sedimentation around 100 cm from 0.02 cm/year to 0.1 cm/yr. In the Densu core, this shift occurred around the year 960 CE whereas in the KETA core sedimentation rates sharply accelerated in recent times, with a mean date of 1996 CE.



258
259

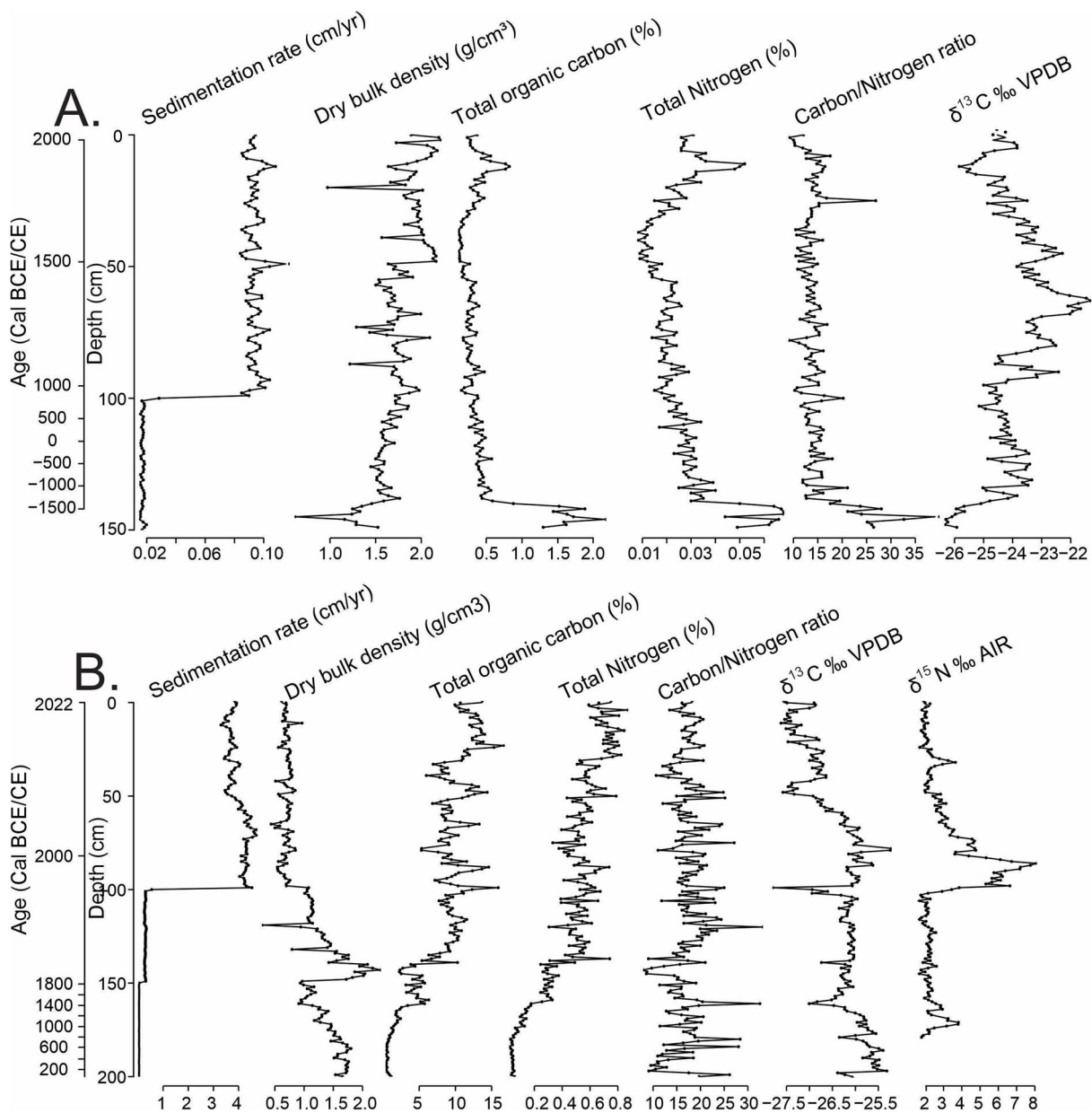
Fig. 2: Age-depth curves of Densu (a) and Keta Cores (b) generated in OxCal version 4.4 (Bronk-Ramsey, 1995; 2009)

262

C, N (C/N), $\delta^{13}\text{C}$, and $\delta^{15}\text{N}$

263
264 Generally, the Densu core shows a decreasing C content upcore (from 2.2% to 0.1%) with
265 values >1% observed between 1384 BCE and 1918 BCE. Like the C, the N content in the Densu
266 core decreases upcore with values ranging from 0.01% to 0.07%. Very low values of 0.01%
267 occur between 1678 CE and 1502 CE while high N values ($N > 0.06\%$) occur between 1440 BCE
268 and 1919 BCE. High C/N in the older regions of the core corresponded with low bulk-density
269 values and vice versa. The C/N ratios decreases upcore (from 39 to 9) in the Densu Core. High
270 C/N values ($C/N > 20$) occur between 1440 BCE and 1919 BCE, varied between 19 and 11
271 between 1384 BCE and 1967 CE, and remained below 10 from 1977 CE to the present.
272 Generally, $\delta^{13}\text{C}$ values increase upcore, varying between -26‰ and -23‰. The N content of
273 the Densu core is too low to measure $\delta^{15}\text{N}$. Largely, the C and N content of the Keta core

274 increase upcore, varying between 1% and 17%, and 0.03% and 0.9% respectively. High C and
 275 N correspond with low bulk density with the later decreasing upcore. Several high peaks
 276 implying huge variabilities in both C and N content were observed in the Keta core.
 277

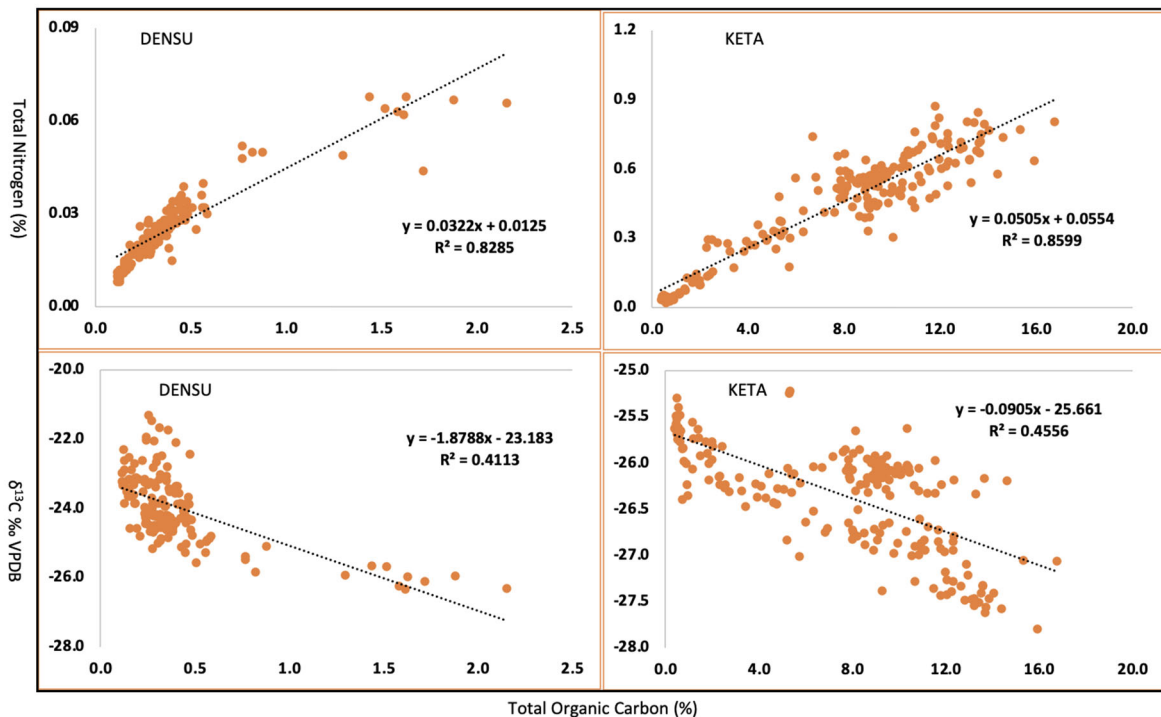


278
 279
 280 Figure 3: Downcore profiles of sedimentation rates, dry bulk density, C, N, C/N ratio, $\delta^{13}\text{C}$
 281 and $\delta^{15}\text{N}$ of the Densu (A) and Keta (B) Cores. Negative ages on the y-axis represent BCE
 282 years.

283
 284 The $\delta^{13}\text{C}$ values in the KETA core decrease upcore from -25‰ and -28‰ with low values
 285 corresponding to C, N, and C/N peaks. The $\delta^{15}\text{N}$ values increase upcore varying between 1.7‰
 286 and 8.1‰ with very high values (i.e., $\delta^{15}\text{N} > 4\text{‰}$) occurring between 2000 CE and 1996 CE. Due
 287 to the very low N content (i.e., $\text{N} < 0.1$) from 758 CE to 62 CE, no $\delta^{15}\text{N}$ was measured in this
 288 part of the core.

289

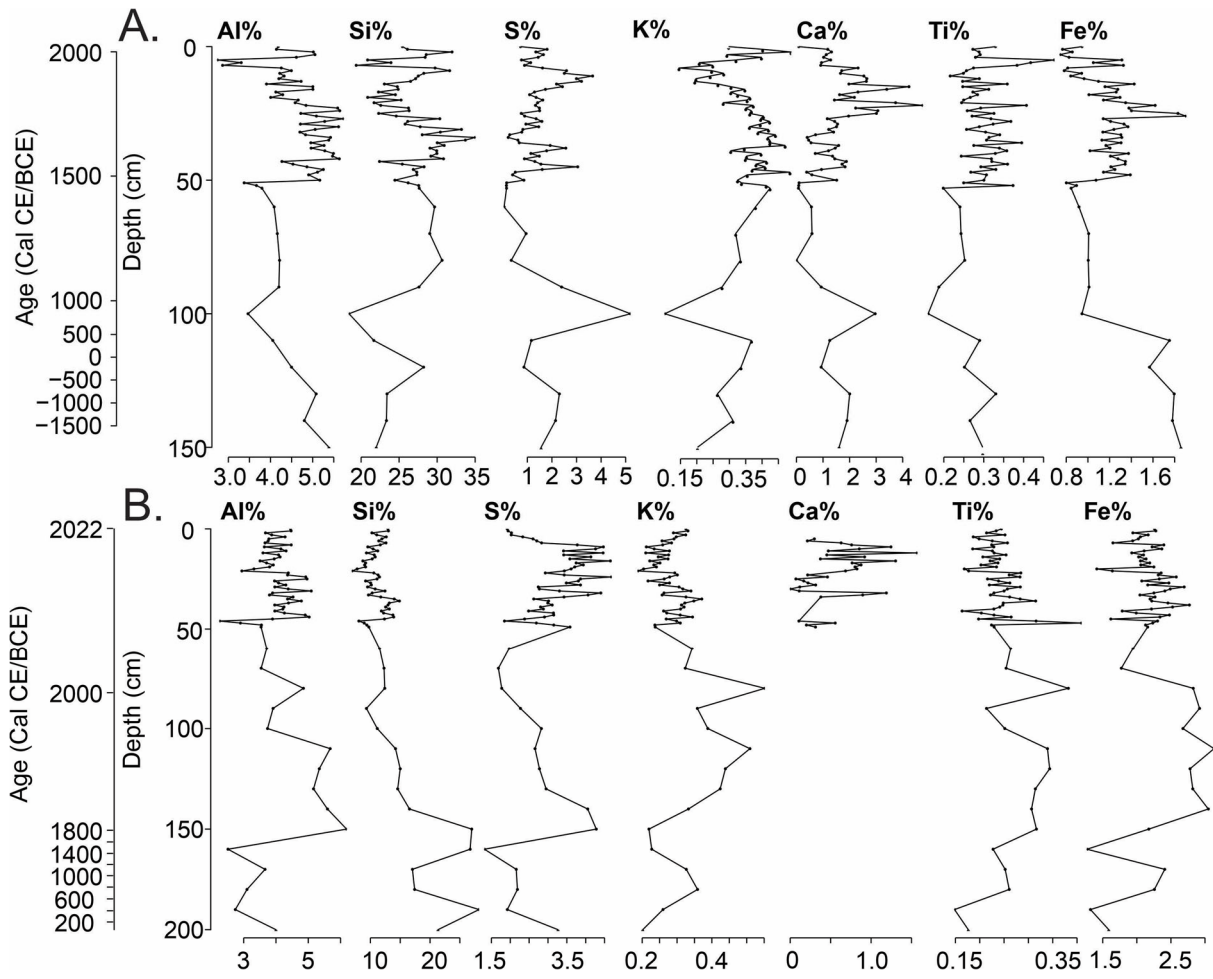
290 The C, N, $\delta^{13}\text{C}$, and $\delta^{15}\text{N}$ data in the Keta core are all comparatively higher than in the Densu
 291 core, except for $\delta^{13}\text{C}$ which increases toward the present and vice versa in the latter. A strong
 292 correlation ($R^2=0.82$ for Densu and $R^2=0.86$ for Keta) exists between N and C in both cores.



293
 294 Figure 4: Relationships between Total Nitrogen (TN), $\delta^{13}\text{C}$, and Total Organic Carbon (TOC) in
 295 sediment cores from Densu (left) and Keta (right) lagoons.
 296

297 Trace Element Geochemistry

298 Both major and minor elements show high variability in both the Densu and Keta cores with
 299 no distinct trends observed upcore or downcore. In the case of the Densu, major element
 300 concentrations varied between 2.7% and 5.8% for Al, 18.4% and 32% for Si, 0.1% and 3.7%
 301 for S, 0.1% and 0.5% for K, 0.1% and 4.8% for Ca, 0.2% and 0.4% for Ti, 0.8% and 1.9% for Fe
 302 (Fig. 5). For the Keta core, major element concentrations vary between 2.3% and 6.2% for Al,
 303 6.9% and 28.2% for Si, 1.3% and 4.7% for S, 0.2% and 0.4% for K, 0.01% and 1.6% for Ca, 0.1%
 304 and 0.4% for Ti, 1.2% and 3.0% for Fe (Fig 5). Generally, the levels of all major elements except
 305 for Ca are higher in the Keta core relative to the Densu core. The minor element profiles
 306 exhibit a high degree of variability down both cores (Fig. 6). Minor elements vary between 14
 307 ppm and 48 ppm for Zn, 18 ppm and 34 ppm for Rb, 129 ppm and 347 ppm for Sr, 77 ppm
 308 and 249 ppm for Zr, and 86 ppm and 457 ppm for Mn (Fig. 6A). The minor element
 309 concentrations in the Keta core vary between 16 ppm and 90 ppm for Zn, 10 ppm and 47 ppm
 310 for Rb, 47 ppm and 67 ppm for Sr, 55 ppm and 215 ppm for Zr, and 74 ppm and 414 ppm for
 311 Mn (Fig 6B). The Densu core has comparatively higher Sr relative to the Keta.

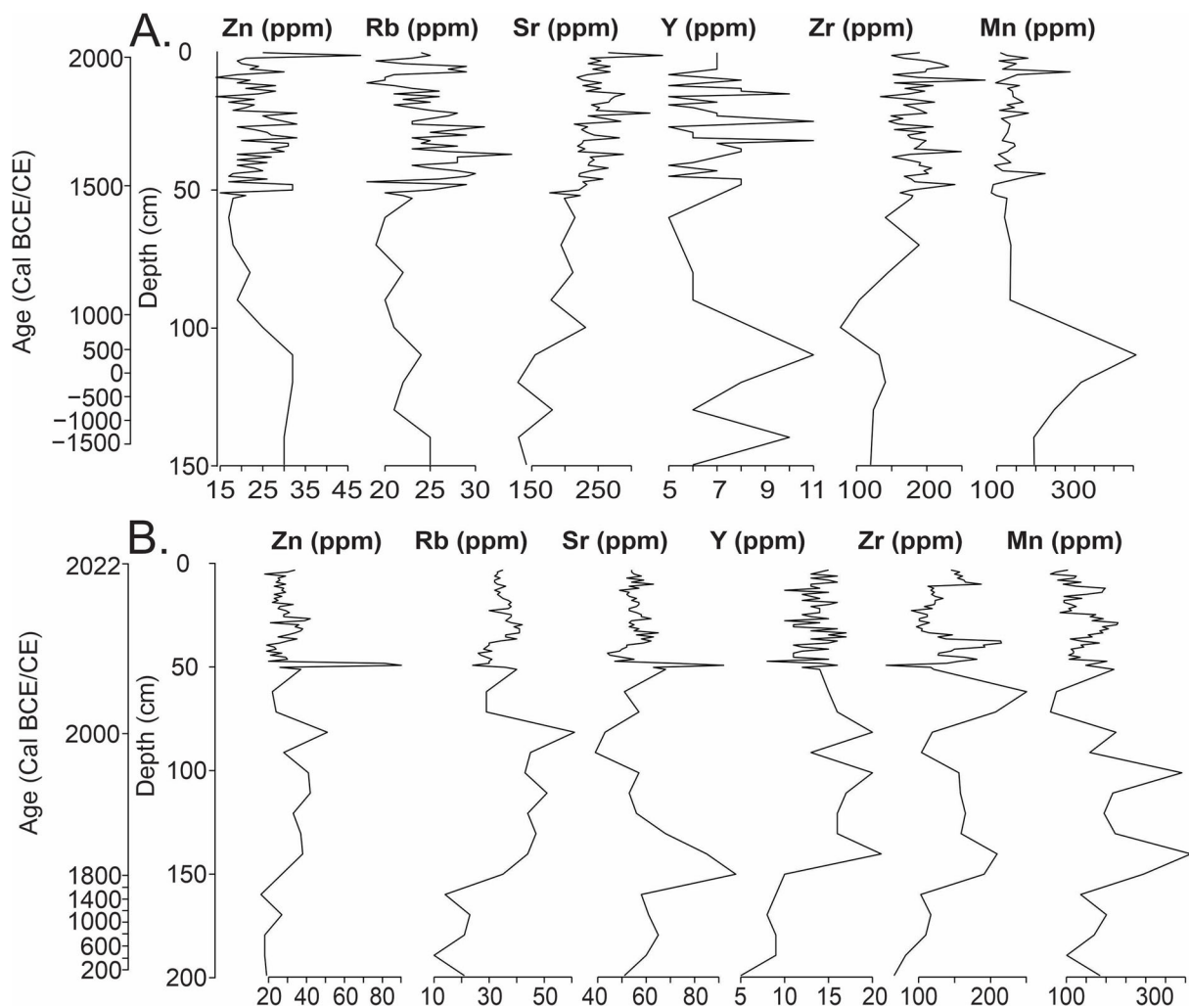


312

313 Figure 5: Downcore profiles of Al, Si, S, Ti, and Fe in the Densu (A) and Keta (B) Cores.

314 Negative ages on the y-axis represent BCE years.

315



317

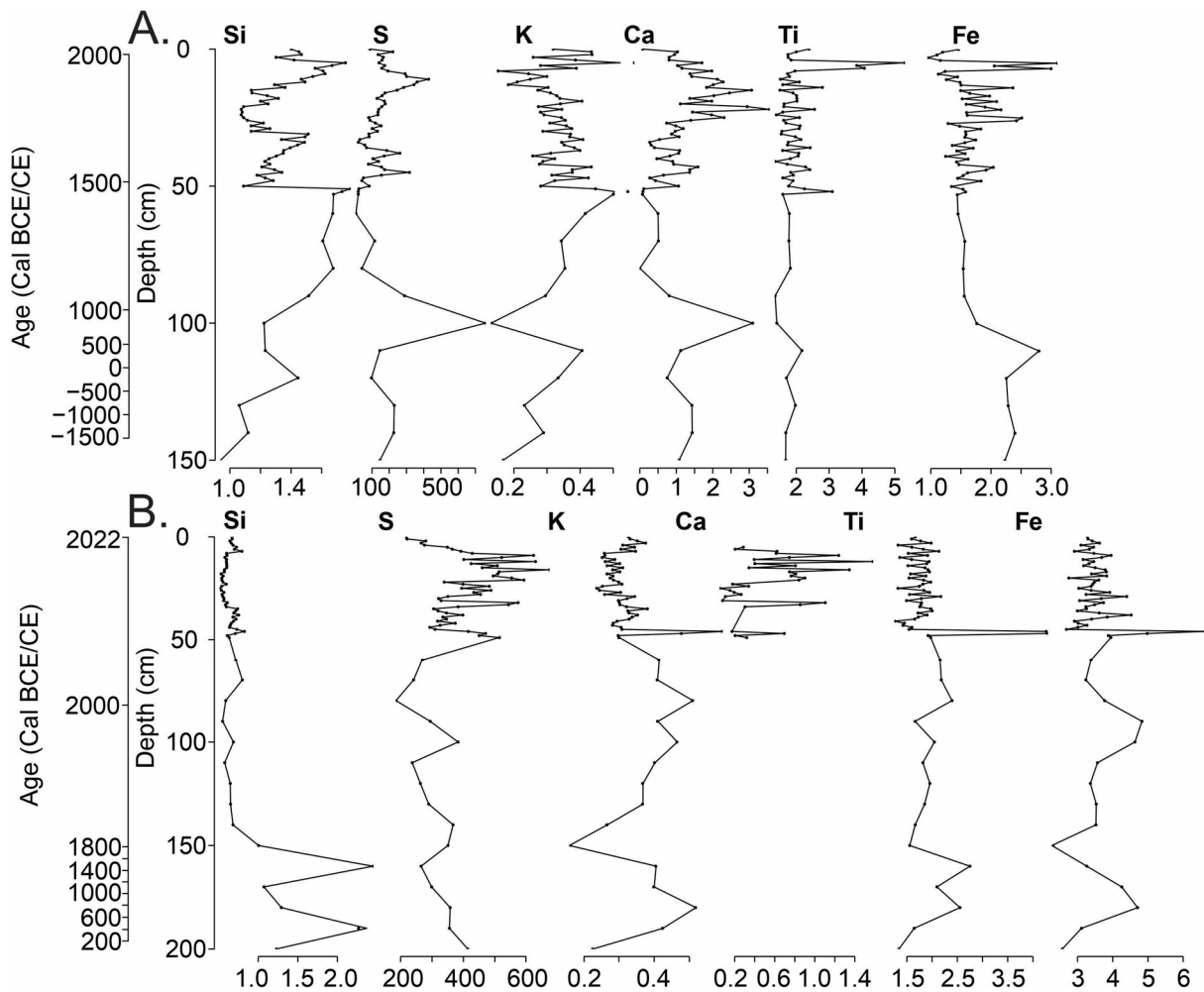
318 Figure 6: Downcore profiles of Zn, Rb, Sr, Y, Zr and Mn in the Densu (A) and Keta (B) cores.
 319 Negative ages on the y-axis represent BCE years.

320

321

322 Trace Element Enrichment Factors

323 The variabilities observed in the concentrations of trace elements in Figures 5 and 6 are likely
 324 due to geochemical effects such as grain size (Liu et al., 2019), and thus may not necessarily
 325 reflect pollution from industrial or mining sources. The level of pollution in the two estuaries
 326 with respect to major and minor elements is explained using the estimated enrichment
 327 factors. The Densu core shows depletion in S and K, depletion to moderate enrichment in Fe,
 328 depletion to significant enrichment in Ti, and significant to extremely high enrichment in S
 329 (Fig. 7). The Keta core, on the other hand, shows depletion in Ca and K, depletion to moderate
 330 enrichment in Si, depletion to significant Ti and Fe, and extremely high enrichment in S (Fig.
 331 7). Although no distinct trends in major elements are observed, high enrichment values have
 332 been observed in recent times. Though both cores show extremely high enrichment in S, the
 333 values are more than ten times higher in some sections of the Keta relative to the Densu.

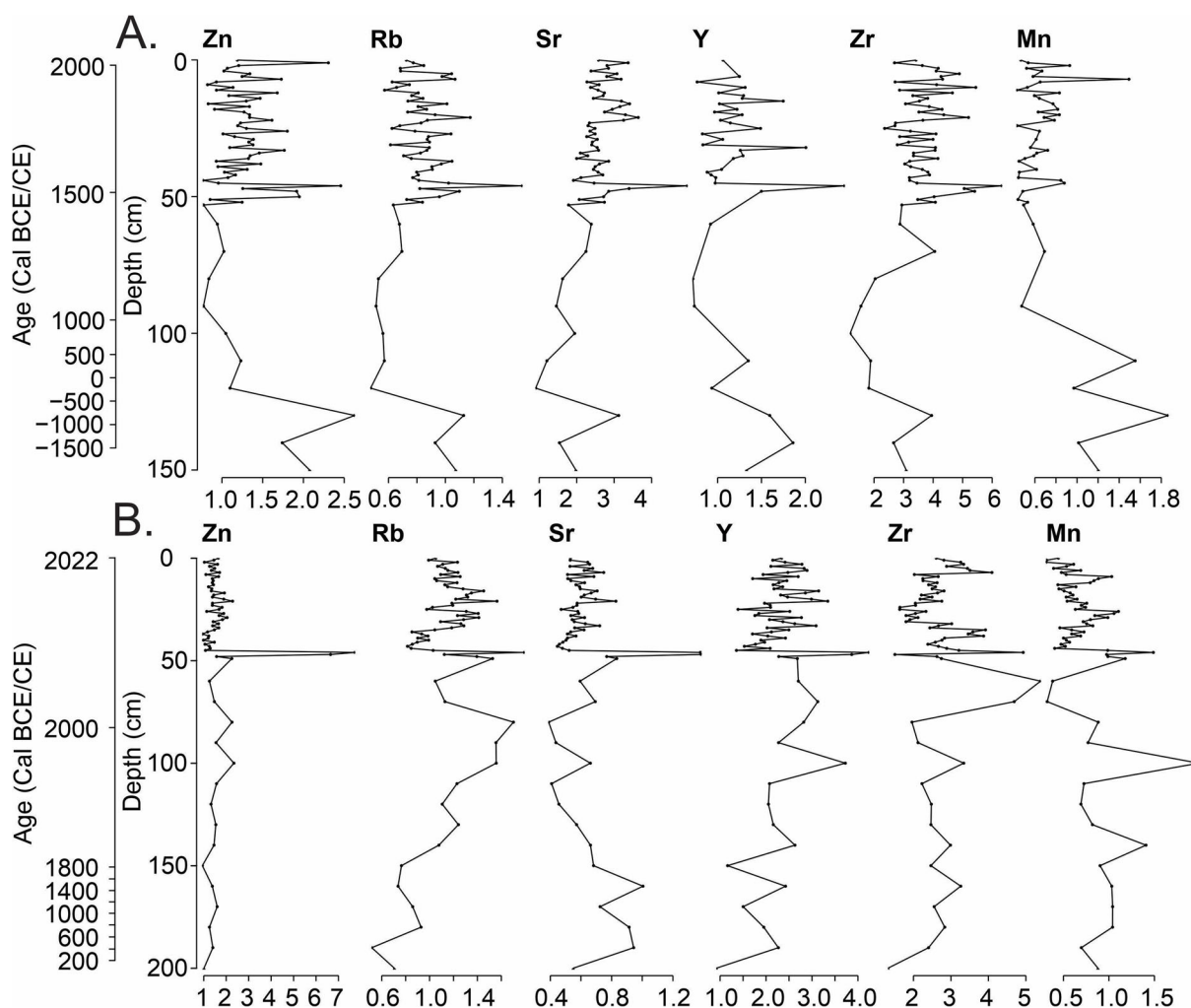


334

335 Figure 7: Profiles of Enrichment Factors for Si, S, K, Ca, Ti, Fe, and La for the Densu (A) and
 336 Keta (B) Cores.

337

338 For minor elements (Fig. 8), the Densu core shows depletion in Rb, and Mn, depletion to
 339 moderate enrichment in Zn and Sr, and depletion to significant enrichment in Zr. The Keta
 340 core, on the other hand, shows depletion in Rb, Mn, and Sr and depletion to significant
 341 enrichment in Zr and Zn. The trends observed in the profiles of enrichment factors for minor
 342 elements are not different from what was observed for the major elements in both cores.



344

345 Figure 8: Profiles of enrichment factors for Zn Rb, Sr, Y, Zr, and Mn in the Densu (A) and Keta
 346 (B). Negative ages on the y-axis represent BCE years.

347

348

349 3. DISCUSSION

350 Radiocarbon Dates and Sedimentation rates.

351 Obtaining reliable chronologies from mangrove sediments is challenging, due to the
 352 complexity of mangrove carbon cycling (Sefton et al., 2021) and the dynamic sedimentary
 353 environment (Peros et al., 2015). The use of ligneous remains and charcoal as dating material
 354 may mean that the dates reported in this study may have been affected by the 'old wood
 355 effect', whereby woody remains and charcoal can be much older than the sediments in which
 356 they are deposited within (Schiffer, 1986). It is difficult to assess the accuracy of these age-
 357 depth models due to these uncertainties, in addition to the limited number of dates available
 358 in the study. Despite these limitations, the models generated show a reasonable agreement
 359 with the data. As well as showing agreement with stratigraphic shifts seen in the profiles of C

360 and N in both cores, these dates provide an interpretative chronological framework for the
361 chemical analysis.

362

363 The sedimentation rate in estuarine environments is partly controlled by the sediment supply,
364 which depends on factors such as climate, the transformation of a river, and its catchment,
365 as well as other processes occurring in the sea (Armitage et al., 2011). While natural events
366 such as floods can significantly affect sedimentation rates, most of the factors are linked to
367 human activities like reclamation, urbanization, industrialization, and deforestation (Godoy
368 et al., 2012; Sanders et al., 2016). Although sedimentation rates were far slower in the Densu
369 core compared with those obtained at Keta, coincidentally, both cores showed a rapid
370 increase in sedimentation rate observed at around 100 cm depth. At first glance, the
371 coincidental alteration in sedimentation rate at the 100 cm mark may be interpreted as
372 stemming from comparable natural or anthropogenic factors influencing the shift in
373 sedimentation regime in both estuaries. However, it is important to note that the two depths
374 represented different ages in both cores. In the case of the Densu core, the rapid shift in
375 sedimentation rate at 100 cm overlaps with the year 960 CE whereas in the KETA the shift at
376 100 cm is more recent occurring around 1996 CE. This suggests that different factors could be
377 driving the sediment inflow and variabilities within the two systems. For the Keta core, we
378 attribute this recent and significant change in sedimentation rate to human-induced
379 alterations in land use and land cover dynamics within the Anloga-Anyanui area, notably the
380 extensive harvesting and trade of mangroves for fuel wood (Aheto et al., 2016; Sekey et al.,
381 2023) and clearing of land for farming purposes (Mahu et al., 2023). During the period from
382 1991 to 2020, a total of 37.6% of mangrove/dense vegetation cover, equivalent to 200.2 km²,
383 was lost in the Keta-Anyanui area (Duku et al 2021). This unusual harvesting of mangroves
384 and the resultant loss in forest coverage has created several kilometers of bare earth within
385 the Creek's catchment, consequently accelerating the influx of sediment into the Creek. In
386 the Densu core, the observed periodic shift in sedimentation rate coincides with a sharp
387 decrease in $\delta^{13}\text{C}$, spikes in $\delta^{15}\text{N}$, and a high C/N ratio at 960 CE, suggesting historical
388 catchment changes arising from either anthropogenically driven land-use change or climatic
389 variations such as extended periods of drought accompanied by flood events. We argue that
390 the latter is a more probable cause of the sedimentation shift in the Densu because
391 population growth and heavy land-use transformation are quite recent dating back to the late
392 90s. On the other hand, significant expansion in the built environment, mainly housing and
393 grey infrastructure during the mid to late 90s within the watershed of Densu coupled with
394 damming of the Densu River is likely the cause of low sedimentation rates observed in recent
395 times in the Densu.

396

397 While oysters occur on sediment beds and have the potential to naturally filter sediments,
398 heavy sediment loads may be detrimental to their growth and survival; in the case of the
399 Anyanui Creek, this rapidly increasing sedimentation rate is likely to pose challenges to oyster

400 feeding, growth, and survival. Several studies have established that heavy sediment loads in
401 estuaries impact oyster larval settlement (Poirier et al., 2021), and impair respiration and
402 feeding rates in juvenile and adult oysters (Loosanoff and Tommers, 1948; Wilber and Clarke,
403 2010; Loosanoff, 1962). Although adult oysters can discern between inert and organic
404 particulates (Gonda-King et al., 2010), at higher levels of siltation and sediment accumulation,
405 they generally reduce valve opening and filtration time, which negatively affects their growth
406 rates (Gonda-King et al., 2010). Sedimentation impacts on bivalves are of broader concern for
407 ecosystem health, wild fisheries, and the associated livelihoods. Unpublished data on
408 historical growth rate of oysters in the Anyanui Creek and Densu Estuary show very slow
409 growth rates in the former compared to the latter with improved growth rates in the latter
410 observed in recent times.

411

412 **C, N (C/N) , $\delta^{13}\text{C}$, and $\delta^{15}\text{N}$**

413 Enhanced C in aquatic ecosystems can be both beneficial and detrimental to benthic
414 organisms (Pearson, 1978). The extremely high levels of C in the Keta core compared to the
415 Densu core align with the high sedimentation rate in the Anyanui Creek which is attributed to
416 intense vegetation cover removal, turning forested lands in the catchment basin bare,
417 particularly in recent years. The C content in aquatic ecosystems is influenced by initial
418 biomass production and subsequent degradation, thus integrating the different processes of
419 organic matter source, delivery routes, depositional, and preservation (Meyers, 2003). High
420 sedimentation rates and increasing grain size inferred from the dry bulk density measurement
421 imply short transport time for the sinking particles, and subsequently, low exposure to water
422 column oxidation resulting in higher preservation of C in the Keta core. Thus, the C content in
423 the sediment could represent a bulk value of organic matter that escaped remineralization
424 during sedimentation and subsequent burial.

425

426 The C/N ratio is important in the discrimination of organic matter sources in aquatic
427 ecosystems. Typically, algae have molar C/N values that are commonly between 4 and 10,
428 whereas vascular land plants, which are protein-poor and cellulose-rich, create organic
429 matter that usually has C/N ratios of 20 and greater (Meyers, 1994). The higher C/N ratio and
430 $\delta^{13}\text{C}$ values in the Keta core, particularly in recent times, depict the dominance of organic
431 matter originating from higher terrestrial plants. The marine algae organic matter dominance
432 observed in the mid-1800s in the Keta core suggests a substantial change in land cover during
433 this period which could have reduced terrestrial and fluvial input, promoting in-estuary tidal
434 production of algal organic matter. The C/N and $\delta^{13}\text{C}$ of the Densu core on the other, show a
435 distinct progression from higher vascular plant dominance (high C/N ratios, lower $\delta^{13}\text{C}$ values)
436 of organic matter from the oldest region of the core to marine algae dominance of organic
437 matter (low C/N ratios, higher $\delta^{13}\text{C}$ values) from 1977 CE to present day. An explanation for
438 this change could be a reduction in land-based or riverine organic matter flux into the Densu
439 estuary through time arising from catchment transformation including deforestation to
440 wetland vegetation degradation to the establishment of a well-built environment (Adjei et al.,

441 2019; Antwi-Agyakwa, 2014). The period coincides with the construction of the Weija Dam in
442 the year 1978 on the Densu River (Kuma and Ashley, 2008). It is obvious from this study how
443 the damming of the Densu River has changed the organic matter dynamics and geochemical
444 outlook of the Densu estuary. The estuary is now totally opened to the adjacent sea with
445 limited freshwater input only when there is dam spillage or precipitation. This gives it near or
446 typical seawater salinities (>25 PSU) during most times of the year. The Keta core on the other
447 hand portrays a system dominated by freshwater influx with little seawater influence with a
448 measured salinity ranging between 5-12 PSU. Salinity is among the most important factors
449 affecting the growth and survival of oysters (Nell and Holliday, 1988; Wang and Li, 2018; Tan
450 and Wong, 1996; Davis, 1958), with changes in salinity regarded as one of the most significant
451 environmental stressors for oysters. In a previous study, a very high vulnerability index of 12
452 estimated for the West African Mangrove oyster *C. tulipa* places it among marine organisms
453 that are highly vulnerable to climate change and climate variability (Mahu et al., 2022).
454 Salinity fluctuations driven by variabilities in precipitation and sea level rise is among the most
455 important exposure factors driving this very high vulnerability score. Though adapted to live
456 in a wide range of salinities from 4 ppt to 50 ppt (Mahu et al., 2022), higher salinities have
457 yielded high feeding, growth, and breeding success in the West African mangrove oysters
458 (Sutton et al., 2012; Yankson, 1990; Sutton and Yankson, 2007). Hence in the case of the Keta-
459 Anyanui Creek, our data on reducing salinity in the Creek is well corroborated by the declining
460 growth rate and large mortalities we are observing in the Creek.

461 The composition of $\delta^{15}\text{N}$ in aquatic sediment can be linked to various factors (in a similar way
462 to $\delta^{13}\text{C}$) including nitrogen source, nutrient cycling processes, organic matter input, redox
463 conditions, changing rates of sedimentation for marine and terrestrial input, and
464 anthropogenic processes (Sweeney and Kaplan, 1980; Sebilo et al., 2019). Terrestrial nitrogen
465 compounds discharged as sewage effluent can be differentiated by $\delta^{15}\text{N}$ from non-sewage-
466 related nitrogen compounds. Redox conditions in sediments, particularly, oxygen availability
467 can influence the $\delta^{15}\text{N}$, with aerobic conditions favoring nitrification, which can result in $\delta^{15}\text{N}$
468 depletion and anaerobic conditions promoting denitrification, leading to $\delta^{15}\text{N}$ enrichment (Ke
469 et al., 2019). Also, sedimentation rates can affect the preservation of organic matter in
470 sediments with higher sedimentation rates implying faster burial of organic material. This
471 preservation of organic matter decreases exposure to oxygen and microbial degradation,
472 maintaining the original $\delta^{15}\text{N}$ signature of the organic matter. While it is difficult to ascertain
473 the exact control on $\delta^{15}\text{N}$ in both cores, the contrasting sedimentation rates in the two cores
474 are likely to play a role in higher $\delta^{15}\text{N}$ enrichment in the Keta core and lower $\delta^{15}\text{N}$ in the Densu
475 core. The high $\delta^{15}\text{N}$ values from the change in sedimentation to the top of the Keta core imply
476 faster burial of organic matter and therefore the high $\delta^{15}\text{N}$ values. Again, from the $\delta^{13}\text{C}$
477 profiles, the Densu core has higher $\delta^{13}\text{C}$ compared to the Keta Core, suggesting more algae-
478 generated organic matter in the former and terrestrial organic matter dominance in the latter.
479 Considering that generally, marine plants tend to have lower $\delta^{15}\text{N}$ compared to terrestrial
480 plants (Hoffman et al., 2008), the variabilities in $\delta^{15}\text{N}$ in both cores provide further evidence

481 of dominant marine-dominated processes in the Densu Estuary and terrestrial-dominated
482 processes in the Anyanui Creek.

483

484 **Trace Element Geochemistry and Enrichment**

485 Sulphur (S) deposition in sediments is higher in eutrophic than in oligotrophic sediments due
486 to higher rates of S reduction, enhanced sedimentation of organic S, and less reoxidation
487 (Holmer and Storkholm, 2001). The extremely high enrichment of S and Fe in both cores
488 suggest potential ongoing reduction processes at various scales at the bottom of both the
489 Densu estuary and the Anyanui Creek. These reduction processes could have created
490 chemical boundaries leading to the enrichment of other trace elements and $\delta^{15}\text{N}$ (described
491 above) in the cores. A study conducted on surface sediments for the Densu Estuary showed
492 high and low enrichments of Fe and Mn respectively in the sediments (Akita et al., 2020). The
493 intensity of the reduction processes in the bottom could trigger other chemical processes
494 such as ocean acidification and hypoxia, which has the potential to induce larvae mortality
495 and retard growth in juveniles and adult oysters (Lemasson et al., 2017; Stevick et al., 2021;
496 Jeppesen et al., 2018). In unpublished data, we consistently find very low dissolved oxygen
497 and anoxic conditions in some parts of the Keta-Anyanui Creek. These low oxygen levels,
498 coupled with high sedimentation rate, high nutrient and organic matter content, and low
499 salinity in the Keta-Anyanui Creek present the oysters with coping and adaptation struggles
500 contributing to the poor growth conditions and increasing mortalities witnessed in the Creek.
501 Also, oysters and bivalves in general have the potential to bioaccumulate trace elements
502 (Rodrigues et al., 2022; Mok et al., 2015; Zhu et al., 2020), implying that oysters in both
503 estuaries may be incorporating more than acceptable levels of trace elements into their
504 tissues. Recent studies on heavy metal accumulation in oyster tissues from some selected
505 estuaries in Ghana including the Densu, reported high levels of heavy metals in the tissues of
506 the oyster (Owusu-Prempeh et al., 2022). This potential of oysters to bioconcentrate trace
507 metals has dire implications for their ecological functioning and ecosystem processes as well
508 as for human health.

509

510

511 **Conclusions**

512 Oyster fisheries support the livelihoods of vulnerable artisanal coastal communities along the
513 West African Coast. In addition, they render a suite of ecosystem services to coastal
514 environments in the region. However, their landings and numbers have declined significantly
515 in the past century. The study documents evidence of changing geochemical conditions in two
516 oyster environments, Densu Estuary and keta-Anyanui Creek in Ghana through high-
517 resolution studies of two sediment cores, highlighting likely impacts to the oyster fishery.

518

519 Rapid shifts in sedimentation rates have occurred in both ecosystems through time, however,
520 in the keta-Anyanui Creek, the change in sedimentation rate was more pronounced, and
521 occurred very recently starting from c.1996 CE to the present. In the case of the Densu

522 estuary, the change in sedimentation rate was comparatively little slower and occurred late
523 in the core at c.960 CE. The shift in sedimentation of the Anyanui Creek coincides with periods
524 of intense land cover change i.e., mangrove degradation and vegetation clearing in the
525 Anloga-Anyanui catchment.

526

527 High organic matter accumulation is observed in the Keta-Anyanui Creek relative to the Densu
528 estuary core with C levels in the former about nine times that observed in the latter. The trend
529 observed in C levels agrees with the sedimentation rate in the Anyanui Creek with C levels
530 increasing up the core. On the contrary, the Densu core shows an increasing C content
531 downcore with high C values corresponding to the oldest parts of the core. The trends in N
532 content are like those observed in C for both cores respectively with C and N showing strong
533 correlations.

534

535 The C/N ratio and $\delta^{13}\text{C}$ values of the Keta core suggest organic matter dominated mainly by
536 wetland vegetation with little algae. The C/N ratio and $\delta^{13}\text{C}$ values of the Densu core show a
537 progression from higher vascular plant dominance of organic matter from the oldest region
538 of the core, followed by mangrove dominance by c.1977 CE, and from then on depicting
539 increasing marine algae to present day. The period of transitioning from mangrove
540 dominance to marine algae dominance coincide with the damming of the Densu River in 1978.
541 This observation in the Densu estuary clearly demonstrates a catchment basin that has
542 witnessed various degrees of transformation possibly starting from massive removal of forest
543 cover to wetland vegetation degradation and the establishment of a well-built environment
544 in present-day.

545

546 Extremely high enrichment in S and moderate to significant enrichment of Fe were observed
547 in both the Keta and Densu cores' though higher in Keta. These elevated levels in metals
548 suggest possible ongoing reduction processes at various scales at the bottom of both the
549 Densu estuary and the Keta-Anyanui Creek, particularly in the latter.

550

551 The changes in sediment geochemistry in both cores reflect ongoing changes in the chemical
552 and physical signatures and consequently the health of these ecosystems at a timescale that
553 has not been documented previously. Broadly, these changes will impact the biodiversity and
554 other services such as fisheries production provided by the two ecosystems. With respect to
555 the oyster fisheries, we show from these geochemical data how this globally threatened
556 fishery is being impacted by changing local environmental conditions. With the poorest
557 conditions i.e., very high sedimentation rate, high organic matter accumulation, high $\delta^{15}\text{N}$,
558 high S, and low oxygen levels and salinity documented in the Keta-Anyanui Creek, we
559 conclude that oysters in this environment face serious coping and adaptation challenges.
560 These challenges are evident in the poor growth rate and population health seen in the oyster
561 fishery in the Keta-Anyanui Creek during the past five decades. The changes observed in the
562 health of both environments are largely driven by various transformations in the catchment

563 basin of the two ecosystems, which in the case of Keta-Anyanui, comprise the harvesting and
564 trading of mangroves as well as clearing of the land for agriculture purposes. Such
565 transformations in the catchment will not only impact the oyster fisheries, rather the impacts
566 will extend to the wider inshore biodiversity and fisheries with wide ramifications to
567 livelihoods and the functioning of this important wetland, RAMSAR, and Key Biodiversity
568 Areas. We recommend management actions that prioritize catchment basin protection,
569 ecosystem restoration, and alternative livelihoods devoid of mangrove trading for coastal
570 communities. Future research should focus on addressing questions on the response of
571 oysters to specific geochemical parameters by looking at their direct or indirect impacts on
572 the health of oyster environments. Studies should also focus on devising coping and
573 adaptation strategies that promote oyster population growth to support livelihoods and
574 enhance ecosystem services.

575

576 **Acknowledgment**

577 The authors are grateful to laboratory technicians at the Department of Marine and Fisheries
578 Sciences at the University of Ghana, the British Geological Survey, and the University of York
579 for their immense support during the laboratory work, particularly Gareth Perry for providing
580 his assistance and expertise towards the uXRF analyses in this study.

581

582 **Ethical Statement**

583 Wk lv#duwfdh#grhv#grw#frqwdlq#dq |#w#g lv#z lk#x#p dq#ru#dq lp d#s duwfls dqw1

584

585 **Funding**

586 This research was funded by The Royal Society through the Future Leaders African
587 Independent Research (FLAIR) Fellowship programme through grant number FLR\R1\201385.

588

589 **Author contribution**

590 **EM** conceptualized, supervised, and received funding for the study as well as participated in
591 field sampling and data analysis, and wrote the main manuscript. **ML** assisted with stable
592 isotope and elemental analysis and review of the main manuscript. **LA** assisted with XRF
593 analysis, modeling of radiocarbon dates, data visualization, and review of the manuscript.
594 **EA** assisted with sample preparation and review of the manuscript. **RM** assisted with study
595 design, supervision of study, and writing of the main manuscript. All authors approved the
596 final manuscript to be submitted.

597

598 **Competing Interest**

599 The authors declare no conflict of interest. The funders had no role in the design of the study;
600 in the collection, analysis, or interpretation of the data; in the writing of the manuscript, or in
601 the decision to publish the results.

602

603

604

605

606 **References**

- 607 Adjei FO, Adjei KA, Obuobie E, et al. (2019) Trends in land use/land cover changes in the Densu
608 River basin and its impact on the Weija reservoirs and the Densu Delta (Sakumo I
609 lagoon) in Ghana. *Journal of Geography and Regional Planning* 12(4): 76-89.
- 610 Aheto DW, Kankam S, Okyere I, et al. (2016) Community-based mangrove forest
611 management: Implications for local livelihoods and coastal resource conservation
612 along the Volta estuary catchment area of Ghana. *Ocean & coastal management* 127:
613 43-54.
- 614 Akita LG, Laudien J and Nyarko E (2020) Geochemical contamination in the Densu estuary,
615 Gulf of Guinea, Ghana. *Environmental Science and Pollution Research* 27: 42530-
616 42555.
- 617 Andersson RA, Meyers P, Hornibrook E, et al. (2012) Elemental and isotopic carbon and
618 nitrogen records of organic matter accumulation in a Holocene permafrost peat
619 sequence in the East European Russian Arctic. *Journal of Quaternary Science* 27(6):
620 545-552.
- 621 Antwi-Agyakwa KT (2014) *Assessing the effect of land use land cover change on Weija*
622 *catchment*.
- 623 Armitage JJ, Duller RA, Whittaker AC, and Allen PA (2011). Transformation of tectonic and
624 climatic signals from source to sedimentary archive *Nat. Geosci.*, 4 pp. 231-235
- 625 Baker S and Mann R (1994) Description of metamorphic phases in the oyster *Crassostrea*
626 *virginica* and effects of hypoxia on metamorphosis. *Marine Ecology Progress Series*
627 104: 91.
- 628 Beck MW, Brumbaugh RD, Airoidi L, et al. (2011) Oyster reefs at risk and recommendations
629 for conservation, restoration, and management. *Bioscience* 61(2): 107-116.
- 630 Bernoux M, Cerri CC, Neill C, et al. (1998) The use of stable carbon isotopes for estimating soil
631 organic matter turnover rates. *Geoderma* 82(1-3): 43-58.
- 632 Brock F, Higham T, Ditchfield P, et al. (2010) Current pretreatment methods for AMS
633 radiocarbon dating at the Oxford Radiocarbon Accelerator Unit (ORAU). *Radiocarbon*
634 52(1): 103-112.
- 635 Capelle DW, Kuzyk ZZA, Papakyriakou T, et al. (2020) Effect of terrestrial organic matter on
636 ocean acidification and CO₂ flux in an Arctic shelf sea. *Progress in Oceanography* 185:
637 102319.
- 638 David E, Tanguy A, Pichavant K, et al. (2005) Response of the Pacific oyster *Crassostrea gigas*
639 to hypoxia exposure under experimental conditions. *The FEBS journal* 272(21): 5635-
640 5652.
- 641 Davis H (1958) Survival and growth of clam and oyster larvae at different salinities. *The*
642 *Biological Bulletin* 114(3): 296-307.
- 643 Duku E, Mattah PAD and Angnuureng DB (2021) Assessment of Land Use/Land Cover Change
644 and Morphometric Parameters in the Keta Lagoon Complex Ramsar Site, Ghana.
645 *Water* 13(18): 2537.
- 646 Gazeau F, Gattuso J-P, Greaves M, et al. (2011) Effect of carbonate chemistry alteration on
647 the early embryonic development of the Pacific oyster (*Crassostrea gigas*). *PloS one*
648 6(8): e23010.
- 649 Gonda-King LM, Keppel AG, Kuschner MA, et al. (2010) The Relation of Sedimentation to
650 Growth Rate in the Eastern Oyster (*Crassostrea virginica*). Publ. St. Mary's College of
651 Maryland.

652 Godoy J.M., Oliveira A.V., Almeida A.C., Godoy M.L.D., Moreira I., Wagener A.R., et al.
653 (2012). Guanabara Bay sedimentation rates based on ²¹⁰Pb dating: reviewing the
654 existing data and adding new data J. Braz. Chem. Soc., 23: 1265-1273.

655 Hoffman JC, Bronk DA and Olney JE (2008) Organic matter sources supporting lower food web
656 production in the tidal freshwater portion of the York River estuary, Virginia. *Estuaries
657 and Coasts* 31: 898-911.

658 Holmer M and Storkholm P (2001) Sulphate reduction and sulphur cycling in lake sediments:
659 a review. *Freshwater Biology* 46(4): 431-451.

660 Hopkinson CS, Buffam I, Hobbie J, et al. (1998) Terrestrial inputs of organic matter to coastal
661 ecosystems: An intercomparison of chemical characteristics and bioavailability.
662 *Biogeochemistry* 43: 211-234.

663 Hua Q, Turnbull JC, Santos GM, et al. (2022) Atmospheric radiocarbon for the period 1950–
664 2019. *Radiocarbon* 64(4): 723-745.

665 Jeppesen R, Rodriguez M, Rinde J, et al. (2018) Effects of hypoxia on fish survival and oyster
666 growth in a highly eutrophic estuary. *Estuaries and Coasts* 41: 89-98.

667 Ke Z, Tan Y, Huang L, et al. (2019) Significantly depleted ¹⁵N in suspended particulate organic
668 matter indicating a strong influence of sewage loading in Daya Bay, China. *Science of
669 the total environment* 650: 759-768.

670 Kennish MJ (2002) Environmental threats and environmental future of estuaries.
671 *Environmental conservation* 29(1): 78-107.

672 Kuma JS and Ashley DN (2008) Runoff estimates into the Weija reservoir and its implications
673 for water supply to Accra, Ghana. *Journal of Urban and Environmental Engineering*
674 2(2): 33-40.

675 Lemasson AJ, Fletcher S, Hall-Spencer JM, et al. (2017) Linking the biological impacts of ocean
676 acidification on oysters to changes in ecosystem services: a review. *Journal of
677 experimental marine biology and ecology* 492: 49-62.

678 Leng, M. J., & Lewis, J. P. (2017). C/N ratios and carbon isotope composition of organic matter
679 in estuarine environments. In K. Weckström, K. Saunders, P. Gell, & G. Skilbeck (Eds.),
680 Applications of Paleoenvironmental Techniques in Estuarine Studies. Springer
681 Netherlands. https://doi.org/10.1007/978-94-024-0990-1_9

682 Liu D, Bertrand S and Weltje GJ (2019) An empirical method to predict sediment grain size
683 from inorganic geochemical measurements. *Geochemistry, Geophysics, Geosystems*
684 20(7): 3690-3704.

685 Loosanoff V (1962) Effects of turbidity on some larval and adult bivalves.

686 Loosanoff VL and Tommers FD (1948) Effect of suspended silt and other substances on rate
687 of feeding of oysters. *science* 107(2768): 69-70.

688 Mahu E, Danso P, Edusei MO, et al. (2023) Impact of agricultural practices on ecosystem
689 health of lagoons: a case study of the Keta Lagoon Complex in Ghana, West Africa.
690 *Environmental Monitoring and Assessment* 195(5): 1-15.

691 Mahu E, Sanko S, Kamara A, et al. (2022) Climate resilience and adaptation in West African
692 oyster fisheries: An expert-based assessment of the vulnerability of the oyster
693 *crassostrea tulipa* to climate change. *Fishes* 7(4): 205.

694 Medina E and Francisco M (1997) Osmolality and $\delta^{13}C$ of leaf tissues of mangrove species
695 from environments of contrasting rainfall and salinity. *Estuarine, Coastal and Shelf
696 Science* 45(3): 337-344.

697 Meyers PA (1994) Preservation of elemental and isotopic source identification of sedimentary
698 organic matter. *Chemical geology* 114(3-4): 289-302.

699 Meyers PA (2003) Applications of organic geochemistry to paleolimnological reconstructions:
700 a summary of examples from the Laurentian Great Lakes. *Organic geochemistry* 34(2):
701 261-289.

702 Mok JS, Yoo HD, Kim PH, et al. (2015) Bioaccumulation of heavy metals in oysters from the
703 southern coast of Korea: assessment of potential risk to human health. *Bulletin of*
704 *environmental contamination and toxicology* 94: 749-755.

705 Montagna P, Palmer TA and Pollack JB (2012) *Hydrological changes and estuarine dynamics*.
706 Springer Science & Business Media.

707 Nell JA and Holliday JE (1988) Effects of salinity on the growth and survival of Sydney rock
708 oyster (*Saccostrea commercialis*) and Pacific oyster (*Crassostrea gigas*) larvae and
709 spat. *Aquaculture* 68(1): 39-44.

710 North E, King D, Xu J, et al. (2010) Linking optimization and ecological models in a decision
711 support tool for oyster restoration and management. *Ecological applications* 20(3):
712 851-866.

713 Owusu-Prempeh N, Awuah KO, Abebrese IK, et al. (2022) *Scientific African*.

714 Patterson HK, Boettcher A and Carmichael RH (2014) Biomarkers of dissolved oxygen stress
715 in oysters: a tool for restoration and management efforts. *PLoS one* 9(8): e104440.

716 Pearson T (1978) Macrobenthic succession in relation to organic enrichment and pollution of
717 the marine environment. *Oceanography and marine biology: an annual review* 16:
718 229-311.

719 Perdue EM and Koprivnjak J-F (2007) Using the C/N ratio to estimate terrigenous inputs of
720 organic matter to aquatic environments. *Estuarine, Coastal and Shelf Science* 73(1-2):
721 65-72.

722 Peros M, Gregory B, Matos F, et al. (2015) Late-Holocene record of lagoon evolution, climate
723 change, and hurricane activity from southeastern Cuba. *The Holocene* 25(9): 1483-
724 1497.

725 Poirier LA, Clements JC, Coffin MR, et al. (2021) Siltation negatively affects settlement and
726 gaping behaviour in eastern oysters. *Marine environmental research* 170: 105432.

727 Raj SM and Jayaprakash M (2008) Distribution and enrichment of trace metals in marine
728 sediments of Bay of Bengal, off Ennore, south-east coast of India. *Environmental*
729 *Geology* 56: 207-217.

730 Ramsey CB (1995) Radiocarbon calibration and analysis of stratigraphy: the OxCal program.
731 *Radiocarbon* 37(2): 425-430.

732 Ramsey CB (2009) Bayesian analysis of radiocarbon dates. *Radiocarbon* 51(1): 337-360.

733 Reimer PJ, Austin WE, Bard E, et al. (2020) The IntCal20 Northern Hemisphere radiocarbon
734 age calibration curve (0–55 cal kBP). *Radiocarbon* 62(4): 725-757.

735 Rodrigues LJ, Blemker SR, Frangos SC, et al. (2022) Bioaccumulation of trace metals in two
736 oyster species from southwest Puerto Rico. *Marine Pollution Bulletin* 178: 113581.

737 Sanders CJ, Santos IR, Maher DT, Breithaupt JL, Smoak JM, Ketterer M, et al. (2016)
738 Examining $^{239} + ^{240}\text{Pu}$, ^{210}Pb and historical events to determine carbon, nitrogen and
739 phosphorus burial in mangrove sediments of Moreton Bay, Australia. *J. Environ.*
740 *Radioact.*, 151 (Part 3) pp. 623-629

741 Sebito M, Aloisi G, Mayer B, et al. (2019) Controls on the isotopic composition of nitrite ($\delta^{15}\text{N}$
742 and $\delta^{18}\text{O}$) during denitrification in freshwater sediments. *Scientific reports* 9(1):
743 19206.

744 Sekey W, Obirikorang KA, Boadu KB, et al. (2023) Mangrove plantation and fuelwood supply
745 chain dynamics in the Keta Lagoon Complex Ramsar Site, Ghana. *Wetlands Ecology*
746 *and Management* 31(1): 143-157.

747 Stevick RJ, Post AF and Gómez-Chiarri M (2021) Functional plasticity in oyster gut
748 microbiomes along a eutrophication gradient in an urbanized estuary. *Animal*
749 *microbiome* 3: 1-17.

750 Sutton A, Yankson K and Wubah D (2012) The effect of salinity on particle filtration rates of
751 the west African mangrove oyster. *Journal of Young Investigators* 24(4): 55-59.

752 Sutton AE and Yankson K (2007) PS 33-161: The effect of salinity on filtration rates of the West
753 African mangrove oyster.

754 Sweeney RE and Kaplan I (1980) Natural abundances of ¹⁵N as a source indicator for near-
755 shore marine sedimentary and dissolved nitrogen. *Marine Chemistry* 9(2): 81-94.

756 Tan S-H and Wong T-M (1996) Effect of salinity on hatching, larval growth, survival and settling
757 in the tropical oyster *Crassostrea belcheri* (Sowerby). *Aquaculture* 145(1-4): 129-139.

758 Taylor SR and McLennan SM (1995) The geochemical evolution of the continental crust.
759 *Reviews of geophysics* 33(2): 241-265.

760 Wallace RB, Baumann H, Grear JS, et al. (2014) Coastal ocean acidification: The other
761 eutrophication problem. *Estuarine, Coastal and Shelf Science* 148: 1-13.

762 Wang T and Li Q (2018) Effects of salinity and temperature on growth and survival of juvenile
763 Iwagaki oyster *Crassostrea nippona*. *Journal of Ocean University of China* 17: 941-946.

764 Wilber D and Clarke D (2010) Dredging activities and the potential impacts of sediment
765 resuspension and sedimentation on oyster reefs. *Proceedings of the Western Dredging*
766 *Association Thirtieth Technical Conference, San Juan, Puerto Rico.*

767 Yankson K (1990) Preliminary studies on the rearing of the West African Mangrove Oyster,
768 *Crassostrea tulipa*, in the laboratory. *Discovery and Innovation* 2(4): 45-51.

769 Zhu X, Qiang L, Shi H, et al. (2020) Bioaccumulation of microplastics and its in vivo interactions
770 with trace metals in edible oysters. *Marine Pollution Bulletin* 154: 111079.

771 Zu Ermgassen PS, Bonačić K, Boudry P, et al. (2020) Forty questions of importance to the policy
772 and practice of native oyster reef restoration in Europe. *Aquatic conservation: marine*
773 *and freshwater ecosystems* 30(11): 2038-2049.

774